DR WEN LUO (Orcid ID : 0000-0002-0621-2886)

Article type : Research Article

Synthesis and Biological Evaluation of Genistein-*O*-alkylamine Derivatives as Potential Multifunctional Anti-Alzheimer Agents

Chen Hong, [a] Hui-yan Guo, [b] Shuai Chen, [b] Jian-wu Lv, [b] Xin Zhang, [b] Ya-cheng Yang, [b] Kang Huang, [c] Yi-juan Zhang, [c] Zhi-yong Tian, [c] Wen Luo, [b,*] Yi-ping Chen, [d,*]

[a] *Huaihe Hospital, Henan University, Kaifeng 475000, China*

[b] *Key Laboratory of Natural Medicine and Immuno-Engineering, Henan University, Kaifeng 475004, China*

[c] *Pharmaceutical College, Henan University, Kaifeng 475004, China*

[d] *School of Pharmaceutical Sciences, Guangxi University of Chinese Medicine, Nanning 530200, China*

This article has been accepted for publication and undergone full peer review but has not been through the copyediting, typesetting, pagination and proofreading process, which may lead to differences between this version and the Version of Record. Please cite this article as doi: 10.1111/cbdd.13414

* Wen Luo: Email luowen83@henu.edu.cn, Tel 086 0371-22864665, Fax 086 0371-22864665

* Yi-ping Chen: Email yipchen2009@foxmail.com, Tel 086 0771-4733943

KEYWORDS

Genistein

Alzheimer's disease

Cholinesterase

Antioxidant

Multifunctional

ABSTRACT

A series of genistein derivatives were synthesized and evaluated as multifunctional anti-Alzheimer agents. The results showed that these derivatives had significant acetylcholinesterase (AChE) inhibitory activity; compound **5a** exhibited the strongest inhibition to AChE with an IC_{50} value (0.034 μM) much lower than that of rivastigmine (6.53 μM). A Lineweaver-Burk plot and molecular modeling study showed that **5a** targeted both the catalytic active site (CAS) and the peripheral anionic site (PAS) of AChE. These compounds also showed potent peroxy scavenging activity and metal chelating ability. The compounds did not show obvious effect on HepG2 and PC12 cell viability at the

concentration of 100 μM. Therefore, these genistein derivatives can be utilized as multifunctional agents for the treatment of AD.

1. INTRODUCTION

Alzheimer's disease (AD), a disastrous and highly prevalent neurodegenerative disorder, is typically characterized by memory deficit and progressive impairment of cognitive functions.[1] Approximately 36 million people worldwide suffer from AD, and the number may surpass 115 million by 2050.[2] The pathogenesis of AD is extrmely complex which involves several factors, such as low levels of the acetylcholine (ACh), aggregation of β-amyloid (Aβ), oxidative damage and metal dysregulation.[3]

ACh, being a major neurotransmitter in the brain, plays a crucial role in learning, memory, cognition and consciousness.[4] The pathogenesis of AD may involve the destruction of the cholinergic neurons in the brain of the AD patients. [5] Currently, the main therapeutic approach in the AD treatment involves the enhancement of the cholinergic neurotransmission by inhibiting cholinesterase (ChE). Four cholinesterase inhibitors such as, tacrine, donepezil, rivastigmine and galantamine have been approved by FDA.[6] However, treatments with ChE inhibitors are palliative in nature, which can improve only the clinical symptoms by modulating a single target, but cannot prevent the progression of the disease.

The multi-target-directed ligands (MTDLs) can simultaneously target multiple pathological processes involved in the neurodegenerative cascade, and treatment with MTDLs can be considered as a better therapeutic strategy than the treatment with ChE inhibitors. [7] MTDLs

can be synthesized by conjugating or fusing two or more bioactive scaffolds for multiple complementary biological activities.[8, 9]

High levels of biometals, like copper, zinc and iron bind to the Aβ peptides and generate toxic Aβ oligomers.[10] Redox-active metal ions, such as Cu^{2+} and Fe^{2+} are also involved in the production of reactive oxygen species (ROS). Excessive ROS causes oxidative stress, which eventually destroys the neuronal networks in AD patients.[11] The progression of AD can be retarded by modulating the biometals, inhibiting Aβ aggregation and eliminating the ROS in the brain of the patients.[12]

Genistein (4',5,7-trihydroxyisoflavone, Fig. 1, A), a polyphenolic isoflavone was isolated from *Genista tinctoria* (commonly known as dyer's broom).[13] The compound possesses a broad range of biological activities, such as estrogenic, antioxidant, anti-inflammatory, antimicrobial and metal chelting activity.[14] Genistein also exhibited neuroprotective effect, and ameliorated learning and memory deficits in AD rat model.[15, 16] The curative potentials of different genistein derivatives (Fig. 1, B, C) [17, 18] against AD have been reported in different scientific studies, and genistein molecule can act as a lead compound to synthesize different other derivatives with anti-AD activity.

As per the previous studies by our research group,[19-21] genistein-polyamine conjugates exhibited potent ChEs inhibition activity and metal chelating ability with low cytotoxicity *in vitro*[22] and thus, can be utilized as potent multifunctional agents for AD therapy. One of our previous research also showed that flavonoid derivatives modified with a five-membered

ring (such as pyrrolidine) possess potent ChE inhibitory activity.[23, 24] Therefore, the present study is aimed at synthesizing a series of genistein derivatives with enhanced pharmacological potential by conjugating with pyrrolidine or imidazole using different lengths of carbon spacers as the linker. Among these derivatives, **3h**–**i** and **5e**–**i** are new and have not been reported previously. Although other compounds have been described in several literature (Supporting Information, Table 1), we were unable to find their ChEs inhibitory, antioxidative data (**3a-g**, **5a-d** and **9a-b**) and ^{1}H NMR, ^{13}C NMR data (**3d**, **5a-d** and **9a**). The strategy for synthesis of genistein derivatives is depicted in Fig. 2.

2. METHODS AND MATEREALS

4.1 Chemistry

Melting points (mp) were determined using an X-6 hot stage microscope and were not corrected. ^{1}H NMR and ^{13}C NMR spectra were recorded with Bruker AV-300 or Bruker AV-400 spectrometer in $CDCl_3$ or DMSO-d_6 at 300 or 400 MHz and 75 or 100 MHz, respectively, using solvent peaks [$CDCl_3$: 7.27 (D), 77.2 (C) ppm; and DMSO-d_6: 2.49 (D), 40 (C) ppm] as internal reference. MS spectra were recorded on a Shimadzu LCMS-2010A instrument with an ESI mass selective detector. Elemental analyses were performed on a Gmbe VarioEL Elemental Instrument. Flash column chromatography was performed with silica gel (200 - 300 mesh) purchased from Qingdao Haiyang Chemical Co. Ltd.

2.2 General procedure for the synthesis of the intermediates 2a-e, 4a-e

A suspension of genistein (2.70 g, 10 mmol), anhydrous K_2CO_3 (1.38 g, 10.0 mmol) in acetone (20 mL), α,ω-dibromoalkane (10.0 mmol) were mixed together and refluxed for 10 h. The solvent was evaporated under reduced pressure, the residue was poured into water, extracted with EtOAc, dried and concentrated under vacuum. The intermediates **2a-e** were crystallized from EtOH, and they were used in the next step without further purification.

The intermediates **4a-e** were synthesized following the previously mentioned procedure for **2a-e**, using 40 mmol of α,ω-dibromoalkane and keeping the quantities/concentrations of other reactants same.

2.3 General procedure for the synthesis of compounds 3a-i, 5a-i

A solution of **2a-e** (1.0 mmol), anhydrous K_2CO_3 (2.5 mmol) in CH_3CN (15 mL) and pyrrolidine or imidazole (1.2 mmol) were mixed together and stirred at 60 °C for 8 h. The solvent was removed under vacuum, the mixture was diluted with $CHCl_3$ and then washed with water and brine. The organic layer was dried over Na_2SO_4, and then concentrated under vacuum. The resulting crude product was purified on a silica gel chromatography using a mixture of CH_2Cl_2/MeOH as eluent.

The compounds **5a-i** were synthesized following the previously mentioned procedure for **3a-i**, using 2.5 mmol of pyrrolidine or imidazole.

*2.3.1 5-hydroxy-3-(4-hydroxyphenyl)-7-(2-(pyrrolidin-1-yl)ethoxy)-4H-chromen-4-one (**3a**)*

White solid (73% yield), ^{1}H NMR (300 MHz, DMSO-d_6) δ 12.94 (s, 1H), 9.66 (s, 1H), 8.37 (s, 1H), 7.39 (d, J = 8.7 Hz, 2H), 6.83 (d, J = 8.7 Hz, 2H), 6.61 (d, J = 2.1 Hz, 1H), 6.37 (d, J = 2.1 Hz, 1H), 4.16 (t, J = 5.7 Hz, 2H), 2.80 (t, J = 5.7 Hz, 2H), 2.53 (t, J = 5.4 Hz, 4H), 1.75 – 1.47 (m, 4H). ^{13}C NMR (75 MHz, DMSO-d_6) δ 180.80, 164.81, 162.18, 157.94, 157.88, 154.73, 130.58, 122.92, 121.50, 115.53, 105.82, 98.79, 93.23, 67.99, 54.40, 23.59. MS (ESI$^+$): m/z: 368.1[M+H]$^+$.

*2.3.2 5-hydroxy-3-(4-hydroxyphenyl)-7-(3-(pyrrolidin-1-yl)propoxy)-4H-chromen-4-one (**3b**)*

White solid (75% yield), ^{1}H NMR (300 MHz, DMSO-d_6) δ12.93 (s, 1H), 9.65 (s, 1H), 8.38 (s, 1H), 7.38 (d, J = 8.1 Hz, 2H), 6.82 (d, J = 8.2 Hz, 2H), 6.62 (d, J = 2.7 Hz, 1H), 6.37 (s, 1H), 4.10 (d, J = 6.6 Hz, 2H), 2.42 (s, 4H), 1.88 (t, J = 6.9 Hz, 2H), 1.67 (s, 4H). ^{13}C NMR (75 MHz, DMSO-d_6) δ 180.82, 165.06, 162.18, 157.93, 154.81, 130.62, 122.92, 121.51, 115.53, 105.78, 98.79, 93.23, 67.33, 54.07, 52.48, 28.39, 23.56. MS (ESI$^+$): m/z: 382.2[M+H]$^+$.

*2.3.3 5-hydroxy-3-(4-hydroxyphenyl)-7-(4-(pyrrolidin-1-yl)butoxy)-4H-chromen-4-one (**3c**)*

White solid (67% yield), ^{1}H NMR (300 MHz, DMSO-d_6) δ 8.39 (s, 1H), 7.39 (d, J = 9.0 Hz, 2H), 6.82 (d, J = 6.0 Hz, 2H), 6.64 (d, J = 6.0 Hz, 1H), 6.39 (d, J = 6.0 Hz, 1H), 4.10 (t, J = 6.0 Hz, 2H), 2.45 – 2.33 (m, 6H), 1.85 – 1.70 (m, 2H), 1.66 (t, J = 6.0 Hz, 4H), 1.62 – 1.51 (m, 2H). ^{13}C NMR (75 MHz, DMSO-d_6) δ 180.84, 165.11, 162.21, 157.98, 157.93, 154.80, 130.61, 122.95,

121.53, 115.55, 105.80, 98.81, 93.28, 68.84, 56.50, 55.57, 54.00, 26.87, 25.12, 23.55, 19.01. MS (ESI^+): m/z: 396.2$[M+H]^+$.

*2.3.4 5-hydroxy-3-(4-hydroxyphenyl)-7-((6-(pyrrolidin-1-yl)hexyl)oxy)-4H-chromen-4-one (**3d**)*

White solid (60% yield), ^1H NMR (300 MHz, DMSO-d_6) δ 12.94 (s, 1H), 9.65 (s, 1H), 8.40 (s, 1H), 7.39 (d, *J* = 6.0 Hz, 2H), 6.82 (d, *J* = 7.5 Hz, 2H), 6.63 (s, 1H), 6.38 (s, 1H), 4.07 (s, 2H), 2.37 (s, 6H), 1.76 – 1.60 (m, 6H), 1.50 – 1.29 (m, 6H). ^{13}C NMR (75 MHz, DMSO-d_6) δ 180.84, 165.11, 162.20, 157.96, 157.93, 154.80, 130.61, 122.95, 121.52, 115.55, 105.79, 98.80, 93.26, 68.94, 56.13, 54.08, 28.82, 27.21, 25.82, 23.52. MS (ESI^+): m/z: 424.2$[M+H]^+$.

*2.3.5 7-(2-(1H-imidazol-1-yl)ethoxy)-5-hydroxy-3-(4-hydroxyphenyl)-4H-chromen-4-one (**3e**)*

White solid (53% yield), ^1H NMR (300 MHz, DMSO-d_6) δ 12.94 (s, 1H), 9.60 (s, 1H), 8.40 (s, 1H), 7.69 (s, 1H), 7.39 (d, *J* = 9 Hz, 2H), 7.25 (s, 1H), 6.90 (s, 1H), 6.82 (d, *J* = 6 Hz, 2H), 6.66 (d, *J* =3 Hz, 1H), 6.42 (d, *J* = 3 Hz, 1H), 4.39 (s, 4H). ^{13}C NMR (75 MHz, DMSO-d_6) δ 180.90, 164.31, 162.26, 157.96, 154.93, 138.13, 130.63, 128.83, 123.04, 121.47, 120.21, 115.56, 106.13, 98.90, 93.48, 68.42, 45.72. MS (ESI^+): m/z: 365.1$[M+H]^+$.

*2.3.6 7-(3-(1H-imidazol-1-yl)propoxy)-5-hydroxy-3-(4-hydroxyphenyl)-4H-chromen-4-one (**3f**)*

White solid (55% yield), ^1H NMR (300 MHz, DMSO-d_6) δ 12.96 (s, 1H), 9.63 (s, 1H), 8.41 (s, 1H), 7.64 (s, 1H), 7.39 (d, *J* = 8.7 Hz, 2H), 7.21 (d, *J* = 1.2 Hz, 1H), 6.90 (t, *J* = 1.2 Hz, 1H), 6.83

(d, *J* = 8.7 Hz, 2H), 6.65 (d, *J* = 2.4 Hz, 1H), 6.41 (d, *J* = 2.1 Hz, 1H), 4.15 (t, *J* = 6.9 Hz, 2H), 4.04 (t, *J* = 6.0 Hz, 2H), 2.19 (t, *J* = 6.6 Hz, 2H). ^{13}C NMR (75 MHz, DMSO-d_6) δ 180.88, 164.76, 162.20, 157.94, 154.90, 137.84, 130.63, 128.93, 122.99, 121.50, 119.85, 115.55, 105.98, 98.88, 93.34, 66.02, 43.27, 30.35. MS (ESI$^+$): m/z: 379.1[M+H]$^+$.

*2.3.7 7-(4-(1H-imidazol-1-yl)butoxy)-5-hydroxy-3-(4-hydroxyphenyl)-4H-chromen-4-one (**3g**)*

White solid (56% yield), ^{1}H NMR (300 MHz, DMSO-d_6) δ 12.95 (s, 1H), 9.67 (s, 1H), 8.41 (s, 1H), 7.65 (s, 1H), 7.38 (d, *J* = 8.1 Hz, 2H), 7.20 (s, 1H), 6.89 (s, 1H), 6.82 (d, *J* = 8.1 Hz, 2H), 6.64 (s, 1H), 6.40 (s, 1H), 4.13 – 3.98 (m, 4H), 1.92 – 1.79 (m, 2H), 1.70 – 1.63 (m, 2H). ^{13}C NMR (75 MHz, DMSO-d_6) δ 180.84, 164.94, 162.19, 157.92, 154.86, 137.72, 130.63, 128.82, 122.93, 121.50, 119.74, 115.54, 105.82, 98.80, 93.30, 68.36, 46.00, 27.65, 25.90. MS (ESI$^+$): m/z: 393.1[M+H]$^+$.

*2.3.8 7-((6-(1H-imidazol-1-yl)hexyl)oxy)-5-hydroxy-3-(4-hydroxyphenyl)-4H-chromen-4-one (**3h**)*

White solid (48% yield), mp 200–202 °C; ^{1}H NMR (300 MHz, DMSO-d_6) δ 12.95 (s, 1H), 9.64 (s, 1H), 8.40 (s, 1H), 7.61 (s, 1H), 7.39 (d, *J* = 9.0 Hz, 2H), 7.16 (s, 1H), 6.87 (s, 1H), 6.82 (d, *J* = 6.0 Hz, 2H), 6.64 (s, 1H), 6.38 (s, 1H), 4.05 (t, *J* = 6.0 Hz, 2H), 3.94 (t, *J* =6.0 Hz, 2H), 1.71 (t, *J* = 6.0 Hz, 4H), 147 – 1.39 (m, 2H), 1.30 – 1.23 (m, 2H). ^{13}C NMR (75 MHz, DMSO-d_6) δ 180.84, 165.07, 162.19, 157.96, 157.92, 154.87, 137.67, 130.64, 128.73, 122.93, 121.51, 119.72, 115.54, 105.78, 98.80, 93.26, 68.83, 46.31, 30.95, 28.69, 26.09, 25.34. MS (ESI$^+$):

m/z: 421.2[M+H]$^+$. Elemental Anal. Calcd for $C_{24}H_{24}N_2O_5$: C, 68.56; H, 5.75; N, 6.66. Found: C, 68.77; H, 5.90; N, 6.45.

*2.3.9 7-((8-(1H-imidazol-1-yl)octyl)oxy)-5-hydroxy-3-(4-hydroxyphenyl)-4H-chromen-4-one (**3i**)*

White solid (46% yield), mp 173–175 °C; ^{1}H NMR (300 MHz, DMSO-d_6) δ 12.95 (s, 1H), 9.67 (s, 1H), 8.40 (s, 1H), 7.61 (s, 1H), 7.38 (d, *J* = 9.0 Hz, 2H), 7.15 (s, 1H), 6.88 – 6.79 (m, 3H), 6.63 (s, 1H), 6.38 (s, 1H), 4.05 (t, *J* = 6.0 Hz, 2H), 3.93 (t, *J* = 6.0 Hz, 2H), 1.73 – 1.66 (q, *J* = 6.9 Hz, 4H), 1.37 – 1.18 (m, 8H). ^{13}C NMR (75 MHz, DMSO-d_6) δ 180.83, 165.09, 162.17, 157.95, 157.92, 154.86, 137.66, 130.63, 128.71, 122.91, 121.50, 119.70, 115.53, 105.76, 98.78, 93.24, 68.91, 46.35, 31.01, 29.06, 28.86, 28.80, 26.32, 25.76. MS (ESI$^+$): m/z: 449.2 [M+H]$^+$. Elemental Anal. Calcd for $C_{26}H_{28}N_2O_5$: C, 69.63; H, 6.29; N, 6.25. Found: C, 69.80; H, 6.12; N, .6.04.

*2.3.10 5-hydroxy-7-(2-(pyrrolidin-1-yl)ethoxy)-3-(4-(2-(pyrrolidin-1-yl)ethoxy)phenyl)-4H-chromen-4-one (**5a**)*

White solid (52% yield), ^{1}H NMR (400 MHz, $CDCl_3$) δ 12.31 (s, 1H), 7.81 (s, 1H), 7.38 (d, *J* = 8.8 Hz, 2H), 6.89 (d, *J* = 8.8 Hz, 2H), 6.35 (d, *J* = 2.0 Hz, 1H), 6.27 (d, *J* = 2.0 Hz, 1H), 4.29 (q, *J* = 4.8 Hz, 4H), 3.39 – 3.33 (m, 2H), 3.33 – 3.28 (m, 2H), 3.20 (s, 4H), 3.13 (s, 4H), 1.98 – 1.93 (s, 8H). ^{13}C NMR (100 MHz, $CDCl_3$) δ 180.78, 176.39, 163.68, 162.69, 157.96, 152.96, 130.29,

123.73, 123.57, 114.72, 106.65, 98.87, 92.75, 65.11, 64.31, 53.94, 53.88, 53.62, 53.49, 23.18, 22.13. MS (ESI^+): m/z: 465.2 $[M+H]^+$.

2.3.11 4.4.2

*5-hydroxy-7-(3-(pyrrolidin-1-yl)propoxy)-3-(4-(3-(pyrrolidin-1-yl)propoxy)phenyl)-4H-chromen-4-one (***5b***)*

White solid (68% yield), ^1H NMR (400 MHz, $CDCl_3$) δ 12.84 (s, 1H), 7.85 (s, 1H), 7.44 (d, *J* = 8.8 Hz, 2H), 6.96 (d, *J* = 8.8 Hz, 2H), 6.40 (d, *J* = 2.0 Hz, 1H), 6.36 (d, *J* = 2.0 Hz, 1H), 4.12 – 4.05 (m, 4H), 2.85 – 2.76 (m, 2H), 2.72 (t, *J* = 6.8 Hz, 6H), 2.64 (s, 4H), 2.14 – 2.07 (m, 4H), 1.89 – 1.83 (m, 8H). ^{13}C NMR (100 MHz, $CDCl_3$) δ 180.81, 164.93, 162.62, 159.12, 157.94, 152.70, 130.09, 123.58, 122.97, 114.65, 106.20, 98.70, 92.80, 66.90, 66.22, 54.23, 53.14, 52.88, 28.31, 28.26, 23.48. MS (ESI^+): m/z: 493.3 $[M+H]^+$.

2.3.12

*5-hydroxy-7-(4-(pyrrolidin-1-yl)butoxy)-3-(4-(4-(pyrrolidin-1-yl)butoxy)phenyl)-4H-chromen-4-one (***5c***)*

White solid (60% yield), ^1H NMR (400 MHz, $CDCl_3$) δ 12.86 (s, 1H), 7.86 (s, 1H), 7.45 (d, *J* = 8.4 Hz, 2H), 6.96 (d, *J* = 8.4 Hz, 2H), 6.39 (d, *J* = 2.0 Hz, 1H), 6.36 (d, *J* = 2.0 Hz, 1H), 4.15 – 3.94 (m, 4H), 3.16 – 2.38 (m, 12H), 1.87 – 1.79 (m, 16H). ^{13}C NMR (100 MHz, $CDCl_3$) δ 180.84, 164.93, 162.64, 159.15, 157.94, 152.72, 130.11, 123.61, 122.86, 114.63, 106.18, 98.55, 92.84, 68.28, 67.61, 55.97, 54.13, 27.15, 26.95, 25.06, 23.42. MS (ESI^+): m/z: 521.3 $[M+H]^+$.

2.3.13

*5-hydroxy-7-((6-(pyrrolidin-1-yl)hexyl)oxy)-3-(4-((6-(pyrrolidin-1-yl)hexyl)oxy)phenyl)-4H-chromen-4-one (***5d***)*

White solid (57% yield), ^{1}H NMR (400 MHz, $CDCl_3$) δ 12.85 (s, 1H), 7.86 (s, 1H), 7.44 (d, *J* = 8.8 Hz, 2H), 6.95 (d, *J* = 8.8 Hz, 2H), 6.38 (d, *J* = 2.2 Hz, 1H), 6.35 (d, *J* = 2.2 Hz, 1H), 4.01 (t, *J* = 5.2 Hz, 2H), 3.98 (t, *J* = 5.2 Hz, 2H), 2.71 (d, *J* = 6.4 Hz, 8H), 2.65 – 2.57 (m, 4H), 1.92 – 1.85 (m, 8H), 1.85 – 1.78 (m, 4H), 1.67 –1.64 (m, 4H), 1.53 – 1.46 (m, 4H), 1.46 – 1.39 (m, 4H). ^{13}C NMR (100 MHz, $CDCl_3$) δ 180.84, 165.06, 162.65, 159.30, 157.96, 152.67, 130.07, 123.62, 122.80, 114.66, 106.15, 98.61, 92.82, 68.51, 67.89, 56.27, 54.07, 54.04, 29.09, 28.83, 28.12, 28.05, 27.22, 27.19, 25.90, 25.83, 23.41. MS (ESI^+): m/z: 577.4 $[M+H]^+$.

2.3.14

*7-(2-(1H-imidazol-1-yl)ethoxy)-3-(4-(2-(1H-imidazol-1-yl)ethoxy)phenyl)-5-hydroxy-4H-chromen-4-one (***5e***)*

White solid (59% yield), mp 85–87 °C; ^{1}H NMR (300 MHz, $CDCl_3$) δ 12.83 (s, 1H), 7.85 (s, 1H), 7.59 (s, 2H), 7.43 (d, *J* = 9 Hz, 2H), 7.05 (d, *J* = 9 Hz, 4H), 6.93 (d, *J* = 6 Hz, 2H), 6.34 (d, *J* = 6 Hz, 2H), 4.35 (t, *J* = 6 Hz, 4H), 4.26 (t, *J* = 6 Hz, 4H). ^{13}C NMR (75 MHz, $CDCl_3$) δ 180.76, 163.63, 162.87, 158.19, 157.80, 152.93, 137.57, 137.52, 130.26, 129.82, 129.62, 123.70, 123.53, 119.37, 119.33, 114.72, 106.66, 98.34, 93.05, 67.64, 67.34, 46.43, 46.11. MS (ESI^+): m/z: 459.2 $[M+H]^+$. Elemental Anal. Calcd for $C_{25}H_{22}N_4O_5$: C, 68.49; H, 4.84; N, 12.22. Found: C, 68.72; H, 4.91; N, 12.32.

2.3.15

*7-(3-(1H-imidazol-1-yl)propoxy)-3-(4-(3-(1H-imidazol-1-yl)propoxy)phenyl)-5-hydroxy-4H-chromen-4-one (***5f***)*

White solid (52% yield), mp 95–97 °C; ^{1}H NMR (300 MHz, $CDCl_3$) δ 12.84 (s, 1H), 7.87 (s, 1H), 7.47 (s, 3H), 7.43 (s, 1H), 7.06 (d, *J* = 3.6 Hz, 2H), 6.95 (d, *J* = 8.7 Hz, 2H), 6.92 (d, *J* = 1.5 Hz, 2H), 6.35 (s, 2H), 4.19 (t, *J* = 6.3 Hz, 4H), 3.94 (q, *J* = 6.0 Hz, 4H), 2.30 – 2.19 (m, 4H). ^{13}C NMR (75 MHz, $CDCl_3$) δ 180.80, 164.26, 162.80, 158.67, 157.95, 152.80, 137.32, 137.27, 130.23, 129.85, 129.68, 123.64, 123.37, 119.01, 118.90, 114.62, 106.55, 98.60, 92.73, 77.26, 64.39, 63.80, 43.41, 43.26, 30.74, 30.47. MS (ESI^+): m/z: 487.2 $[M+H]^+$. Elemental Anal. Calcd for $C_{27}H_{26}N_4O_5$: C, 66.66; H, 5.39; N, 11.52. Found: C, 66.43; H, 5.57; N, 5.09.

2.3.16

*7-(4-(1H-imidazol-1-yl)butoxy)-3-(4-(4-(1H-imidazol-1-yl)butoxy)phenyl)-5-hydroxy-4H-chromen-4-one (***5g***)*

White solid (48% yield), mp 104–106 °C; ^{1}H NMR (300 MHz, $CDCl_3$) δ 12.85 (s, 1H), 7.86 (s, 1H), 7.50 (s, 2H), 7.44 (d, *J* = 8.4 Hz, 2H), 7.07 (s, 2H), 6.94 (d, *J* = 4.5 Hz, 4H), 6.35 (d, *J* = 6.3 Hz, 2H), 4.06 – 3.98 (m, 8H), 2.04 –1.95 (m, 4H), 1.86 – 1.74 (m, 4H). ^{13}C NMR (75 MHz, $CDCl_3$) δ 180.82, 164.61, 162.76, 158.96, 157.93, 152.72, 137.11, 130.17, 129.72, 129.61, 123.63, 123.08, 118.77, 118.72, 114.60, 106.33, 98.48, 92.81, 67.73, 67.18, 46.75, 46.68, 28.08, 27.93, 26.26, 26.08. MS (ESI^+): m/z: 515.3 $[M+H]^+$. Elemental Anal. Calcd for $C_{29}H_{30}N_4O_5$: C, 67.69; H, 5.88; N, 10.89. Found: C, 67.53; H, 5.61; N, 11.00.

2.3.17

*7-((6-(1H-imidazol-1-yl)hexyl)oxy)-3-(4-((6-(1H-imidazol-1-yl)hexyl)oxy)phenyl)-5-hydroxy-4H-chromen-4-one (***5h***)*

White solid (50% yield), mp 87–89 °C; ^{1}H NMR (300 MHz, $CDCl_3$) δ 12.85 (s, 1H), 7.85 (s, 1H), 7.45 (d, *J* = 3.6 Hz, 3H), 7.42 (s, 1H), 7.05 (s, 2H), 6.95 (s, 1H), 6.91 (d, *J* = 6.9 Hz, 3H), 6.35 (d, *J* = 7.2 Hz, 2H), 4.01 – 3.92 (m, 8H), 1.84 – 1.76 (m, 8H), 1.51 – 1.45 (m, 4H), 1.41 – 1.33 (m, 4H). ^{13}C NMR (75 MHz, $CDCl_3$) δ 180.82, 164.94, 162.74, 159.22, 157.95, 152.62, 137.05, 130.10, 129.48, 129.43, 123.67, 122.89, 118.74, 114.66, 106.22, 98.54, 92.84, 68.28, 67.70, 46.94, 31.03, 31.00, 29.01, 28.77, 26.31, 26.30, 25.62, 25.56. MS (ESI^+): m/z: 571.3 $[M+H]^+$. Elemental Anal. Calcd for $C_{33}H_{38}N_4O_5$: C, 69.45; H, 6.71; N, 9.82. Found: C, 69.59; H, 6.39; N, 9.73.

2.3.18

*7-((8-(1H-imidazol-1-yl)octyl)oxy)-3-(4-((8-(1H-imidazol-1-yl)octyl)oxy)phenyl)-5-hydroxy-4H-chromen-4-one (***5i***)*

White solid (43% yield), mp 75–77 °C; ^{1}H NMR (300 MHz, $CDCl_3$) δ 12.85 (s, 1H), 7.85 (s, 1H), 7.43 (d, *J* = 9.6 Hz, 4H), 7.05 (s, 2H), 6.95 (d, *J* = 8.4 Hz, 2H), 6.90 (s, 2H), 6.36 (d, *J* = 7.5 Hz, 2H), 4.02 – 3.90 (m, 8H), 1.77 (t, *J* = 7.2 Hz, 8H), 1.46 – 1.24 (m, 16H). ^{13}C NMR (75 MHz, $CDCl_3$) δ 180.84, 165.04, 162.66, 159.29, 157.94, 152.64, 137.09, 130.07, 129.40, 123.64, 122.76, 118.78, 114.64, 106.14, 98.56, 92.83, 68.54, 67.93, 47.03, 31.08, 29.17, 29.14, 29.02, 28.88, 26.50, 25.93, 25.85. MS (ESI^+): m/z: 626.4 $[M+H]^+$. Elemental Anal. Calcd for $C_{37}H_{46}N_4O_5$: C, 70.90; H, 7.40; N, 8.94. Found: C, 70.82; H, 7.68; N, 9.08.

2.4 Synthesis of compounds 9a-b

The intended compounds **9a-b** were obtained following the literature reported procedure,[25] as shown in the Scheme 2.

*2.4.1 3-(4-(4-(diethylamino)butoxy)phenyl)-5,7-dihydroxy-4H-chromen-4-one (**9a**)*

^{1}H NMR (300 MHz, DMSO-d_6) δ 12.91 (s, 1H), 11.06 (s, 1H), 10.39 (s, 1H), 8.36 (s, 1H), 7.50 (d, J = 8.1 Hz, 2H), 7.01 (d, J = 8.4 Hz, 2H), 6.45 (d, J = 2.1 Hz, 1H), 6.28 (d, J = 2.1 Hz, 1H), 4.06 (t, J = 5.7 Hz, 2H), 3.12 –3.07 (m, 6H), 1.89 – 1.77 (m, 4H), 1.23 (t, J = 7.2 Hz, 6H). ^{13}C NMR (75 MHz, DMSO-d_6) δ 180.55, 164.95, 162.38, 158.82, 158.00, 154.76, 130.64, 123.47, 122.34, 114.71, 104.85, 99.54, 94.22, 67.36, 50.61, 46.47, 26.29, 20.43, 8.88. MS (ESI$^+$): m/z: 398.2 $[M+H]^+$.

*2.4.2 5,7-dihydroxy-3-(4-(4-(pyrrolidin-1-yl)butoxy)phenyl)-4H-chromen-4-one (**9b**)*

^{1}H NMR (400 MHz, DMSO-d_6) δ 12.92 (s, 1H), 11.05 (s, 1H), 10.73 (s, 1H), 8.37 (s, 1H), 7.49 (d, J = 8.8 Hz, 2H), 7.00 (d, J = 8.8 Hz, 2H), 6.43 (d, J = 2.0 Hz, 1H), 6.27 (d, J = 2.0 Hz, 1H), 4.03 (t, J = 5.6 Hz, 2H), 3.56 – 3.47 (m, 2H), 3.18 – 3.13 (m, 2H), 2.98 – 2.93 (m, 2H), 1.98 (s, 2H), 1.86 – 1.78 (m, 6H). ^{13}C NMR (100 MHz, DMSO-d_6) δ 180.56, 164.94, 162.40, 158.83, 158.02, 154.77, 130.64, 123.47, 122.36, 114.73, 104.87, 99.54, 94.22, 67.33, 53.99, 53.26, 26.32, 23.15, 22.57. MS (ESI$^+$): m/z: 396.2 $[M+H]^+$.

2.5 Biological activity

2.5.1 Inhibition assays on AChE and BuChE in vitro

AChE (E.C. 3.1.1.7, from *electric eel*), BuChE (E.C. 3.1.1.8, from *equine serum*), 5,5'-dithiobis-(2-nitrobenzoic acid) (DTNB), acetylthiocholine chloride (ATC), butylthiocholine chloride (BTC) were purchased from Sigma-Aldrich. The compounds were dissolved in a minimum volume of DMSO (1%) and diluted in phosphate-buffered solution (0.1 M, pH 8.0) to provide a final concentration range. All the assays were under the phosphate-buffered solution, using a Shimadzu UV-2450 Spectrophotometer. Enzyme solutions were prepared to give 2.0 units/mL in 2 mL aliquots. The assay medium contained 10 μL of enzyme, 50 μL of DTNB (0.01 M) and 50 μL of substrate (ATC, 0.01 M). The substrate was added to the assay medium containing enzyme, buffer, and DTNB with inhibitor after 15 min of incubation time at 37 °C. The activity was determined by measuring the increase in absorbance at 412 nm at 1 min intervals at 37 °C. Calculations were performed according to the method of the equation in Ellman et al.[26] *In vitro* BuChE assay use the similar method described above. Each concentration was assayed in triplicate.

2.5.2 Kinetic characterization of AChE inhibition

Three different concentrations of substrate were mixed in the 1.0 mL phosphate buffer (0.1 M, pH 8.0), containing 50 μL of DTNB, 10 μL AChE, and 50 μL substrate. Test compound was added into the assay solution and pre-incubated with the enzyme at 37°C for 15 min, followed by the addition of substrate. Kinetic characterization of the hydrolysis of ATC

catalyzed by AChE was done spectrometrically at 412 nm. A parallel control with no inhibitor in the mixture, allowed adjusting activities to be measured at various times.

2.5.3 Molecular modeling

The crystal structure of the torpedo AChE (code ID: 1ACJ) were obtained in the Protein Data Bank after eliminating the inhibitor and water molecules. The 3D structure of **5a** was built and performed geometry optimization by molecular mechanics. Further preparation of substrates included addition of Gasteiger charges, removal of hydrogen atoms and addition of their atomic charges to skeleton atoms, and finally, assignment of proper atomic types. Autotors was then used to define the rotatable bonds in the ligand.

Docking studies were carried out using the AutoDock 4.2 program (The Scripps Research Institute, San Diego, CA, USA). The resulting enzyme structure was used as an input for the AutoGrid program. AutoGrid performed a pre-calculated atomic affinity grid maps for each atom type in the ligand plus an electrostatics map and a separate desolvation map present in the substrate molecule. All maps were calculated with 0.375 Å spacing between grid points. The center of the grid box was placed at the bottom of the active site gorge (AChE [2.781 64.383 67.971]. The dimensions of the active site box were set at 50 × 50 × 50 Å. Flexible ligand docking was performed for the compounds. Each docked system was performed by 100 runs of the AutoDock search by the Lamarckian genetic algorithm (LGA). Other than the referred parameters above, the other parameters were accepted as default.

Flexible ligand docking was performed for the compounds. Docking calculations were

carried out using the Lamarckian genetic algorithm (LGA) and all parameters were the same for each docking, the best 10 poses of molecules were retained. After docking, the geometry of resulting complex was studied using the PyMOL program.

2.5.4 Measurement of the anti-oxidation activity

The antioxidation activity was determined by using the oxygen radical absorbance capacity-fluorescein (ORAC-FL) assay. The ORAC-assay measures antioxidant scavenging activity against peroxyl radical induced by 2,2'-azobis(2-amidinopropane) dihydrochloride (AAPH) at 37 °C. The reaction was carried out in 75 mM phosphate buffer (pH 7.4), and the final reaction mixture was 200 μL. Antioxidant (20 μL) and fluorescein (120 μL, 300 nM final concentration) were placed in the wells of a black 96 well plate, and the mixture was incubated for 15 min at 37 °C. Then AAPH solution (60 μL, 12 mM final concentration) was added rapidly. The plate was immediately placed into a Spectrafluor Plus plate reader (BMG, German), and the fluorescence was measured every 60 seconds for 180 minutes with exitation at 485 nm and emission at 535 nm. 6-Hydroxy-2,5,7,8-tetramethylchroman-2-carboxylic acid (Trolox) was used as a standard (1-5 μM, final concentration). A blank (FL+AAPH) using phosphate buffer instead of antioxidant and Trolox calibration were carried out in each assay. The samples were measured at different concentrations (1-5 μM), and at least three independent runs were performed for each sample. The ORAC values calculated as previously described.[21]

2.5.5 MTT assay of HepG2 and PC12 cell viability

MTT assay of PC12 and HepG2 was conducted according to the previous report.[24]

2.5.6 Metal-chelating study

The chelating studies were made in methanol using a Shimadzu UV-2450 Spectrophotometer. The absorption spectrum of test compounds (20 μM), alone or in the presence of $FeCl_3$, $CuSO_4$ or $ZnCl_2$ (20 μM) was recorded with wavelength ranging from 200 to 500 nm after incubating for 30 min at room temperature. The final volume of reaction mixture was 1.0 mL, and the final concentrations of tested compounds and metals were 20 μM. The molar ratio method was performed to determine the stoichiometry of the complex compound-metal by titrating the methanol solution of the compounds with ascending of $CuCl_2$. The final concentration of the compounds was 20 μM, and the final concentration of Cu^{2+} ranged from 2.0 to 200 μM. The spectra was recorded and treated by numerical subtraction of $CuCl_2$ and the compounds at corresponding concentrations, plotted versus the mole fraction of the test compounds.

The complex formation constant (β_1) was calculated as: $\beta_1 = [ML]/[M][L] = (A/A_0)/\{[1-(A/A_0)]^2 \cdot c\}$, where A is the absorption in the curve at the molar ratio of 0.98, A_0 is the absorption at intersection of the two lines (Fig. 5), c is the concentration of the test compound (20 μM).

3. RESULTS AND DISCUSSION

3.1 Chemistry

The 4'-OH group in genistein molecule is more nucleophilic than 7-OH and 5-OH group, but less acidic than 7-OH group, and thus 4'-OH or/and 7-OH can be easily substituted by desired substituents.[27, 28] The intended compounds (**3a–i**, **5a-i**) were synthesized following the synthetic route as depicted in the Scheme 1.

The intermediates **2a-e** and bis-substituted intermediates **4a-e** were synthesized in the presence of excess anhydrous K_2CO_3 by alkylating genistein **1** with equivalent amount dibromoalkanes and 4× equivalent of dibromoalkanes in acetone, respectively for 10 h. The reaction did not produce the tri-substituted compounds as the 5-OH group was stabilized by hydrogen bonds. Finally, **2a-e** or **4a-e** were conjugated with pyrrolidine or imidazole to obtain the intended compounds **3a**-**i** and **5a-i** with satisfactory yields. We also synthesized **GS-14** (Fig. 1, B) and two of 4'-*O*-modified genistein derivatives **9a-b** to calculate the complete structure-activity relationships (SAR) of these series of compounds. While synthesizing the compounds **9a-b**, the 7-OH group of genistein was protected with chloromethyl methyl ether (MOM-Cl) (Scheme 2),[29] and the protected intermediate **6** was alkylated with the equivalent amount of 1,4-dibromobutane in the presence of excess K_2CO_3 in acetone to obtain the intermediate **7**, which in turn was conjugated with diethylamine or pyrrolidine to yield the corresponding intermediates **8a** and **8b**, respectively. Finally, the MOM protecting groups were detached by hydrolyzing with 4 M HCl at room temperature

to obtain the corresponding compounds **9a** and **9b** as hydrochloride salts. The structure and purity of these synthesized new compounds were confirmed by ^{1}H NMR, ^{13}H NMR, ESI-MS and elemental analysis.

3.2 *In vitro* AChE and BuChE inhibition studies

The synthesized compounds (**3a**-**i**, **5a**-**i**, **9a-b** and **GS-14**) were screened for AChE and BuChE inhibitory activities *in vitro* according to the Ellman method. Donepezil and rivastigmine were used as positive controls. The IC_{50} values and selectivity ratio for AChE and BuChE inhibition are summarized in Table 1. The synthesized compounds showed different inhibitory activities towards AChE with their IC_{50} values ranging from the nanomolar to micromolar range (IC_{50} 0.034 – 7.25 μM), and exhibited better inhibition selectivity towards AChE than BuChE. Compound **5a** was obtained as the most potent AChE inhibitor (IC_{50} = 0.034 μM) with a potency of about 200-fold higher than rivastigmine (IC_{50} = 6.53 μM) and 10-fold higher than a reported compound **GS-14** (IC_{50} = 0.29 μM).

The pyrrolidine conjugated compounds (**3a-d**, **5a-d**) exhibited higher potencies (IC_{50} = 0.034 – 1.11 μM) than the positive control, rivastigmine (IC_{50} = 6.53 μM). While most of the imidazole conjugated derivatives (**3e-i** and **5g-i**) did not exhibit effective AChE inhibitory activity with IC_{50} values more than 10 μM. The results indicated that *O*-alkyl-pyrrolidino genistein (but not the imidazole substituted genistein) exhibited significant AChE inhibitory activity, which signifies that the pyrrolidine moiety is crucial for AChE inhibition. On the other hand, imidazole conjugated derivatives **5e** and **5f** (n=2, 3) displayed stronger

inhibitory activity than **5g-i**, the results indicated that the potency of the derivatives to inhibit AChE was related to the length of alkylene. In general, two methylene groups (**3a**, **5a**, **5e**) between genistein and pyrrolidine/imidazole constituted the optimal chain length for this series.

The 4'-O-substituted genistein derivatives **9a-b** showed moderate inhibitory activity (IC_{50}= 4.98, 7.25 μM) compared with **GS-14** (7-O-substituted, IC_{50}= 0.29 μM), **3c** (7-O-substituted, IC_{50}= 0.44 μM) and **5c** (7,4'-O-substituted, IC_{50}= 0.08 μM). The derivatives exhibited AChE inhibition potencies in the following order: 7,4'-O-substituted > 7-O-substituted > 4'-O-substituted genistein derivatives.

BuChE is considered as a potential target for AD therapy owing to its crucial role in regulating acetylcholine levels.[30] The pyrrolidine substituted derivatives (except **3b**, **3c**) exhibited higher BuChE inhibitory activities than rivastigmine (IC_{50} = 1.41 μM). The 7,4'-O-pyrrolidino compounds **5a** and **5c** exhibited the strongest BuChE inhibition with IC_{50} values of 0.33 and 0.35 μM, respectively. The concurrent inhibition of both AChE and BuChE can provide additional benefits in AD therapy (eg. rivastigmine). [31] The present study showed that the compounds **3a-d**, **5a**-**d** can significantly inhibit both AChE and BuChE enzymes.

3.3 Kinetic characterization of AChE inhibition

The most potent AChE inhibitor (**5a**) was selected for kinetic analysis to characterize the inhibition mechanism (Fig. 3, left). Lineweaver-Burk plots showed both increasing slopes and increasing intercepts with higher inhibitor concentration, indicating a mixed-type inhibition.

These results indicate the ability of the compound **5a** to interact with both catalytic active site (CAS) and peripheral anionic site (PAS) of AChE.

3.4 Molecular modeling study

Molecular modeling was carried out by Autodock 4.2 package and PyMOL program[32, 33] to obtain the functional and structural insight into the bond/interaction between the compound **5a** and *Tc*AChE (PDB code: 1ACJ). After docking, the best pose of molecule was chosen and the geometry of complex was studied. (The affinity was shown in Supporting Information, Table 2) The docking result (Fig. 3, right) demonstrated multiple binding modes between **5a** and *Tc*AChE. In the **5a**-*Tc*AChE complex, **5a** occupied the entire enzymatic CAS, mid-gorge and PAS. The pyrrolidine moiety was bound to CAS with cation-π interaction between Trp84 and Phe330; the distance was 3.5 and 3.7 Å, respectively. At the midgorge recognition site, the chromone moiety displayed H-bond with Tyr70, and the distance was 3.2 Å. Another pyrrolidine moiety was bound to PAS with hydrophobic interaction. The docking result showed that the compound **5a** could bind to both CAS and PAS of AChE, and this finding was consistent with the results of the kinetic study.

3.5 Studies of antioxidation activity

The antioxidant activities of the synthesized compounds were evaluated by oxygen radical absorbance capacity (ORAC) assay. Trolox (a vitamin E analogue) was used as the

standard and the antioxidative capacity of the compounds were represented as a Trolox equivalent. Genistein was also tested, with an ORAC value of 4.20 trolox equivalents. All of the target compounds demonstrated weak to moderate antioxidant activity with ORAC values ranging from 0.56 to 2.31 Trolox equivalents (Table 1). Compounds **3e** showed the most potent antioxidant activity (ORAC value = 2.31), whereas compounds **3a**, **3b**, **3f**, **3h** and **GS-14** exhibited slightly lower activities (ORAC value = 1.85, 1.94, 2.13, 2.04 and 2.15, respectively). The 7,4'-*O*-substituted derivatives **5a-5i** showed weak antioxidant activities with ORAC value ranging from 0.56 to 1.23. Donepezil and rivastigmine exhibited minimum free radical scavenging activities with ORAC values < 0.2. These results indicated that the free 4'-OH of genistein was crucial for the free radical scavenging activity.

3.6 Metal-chelating study

High levels of redox-active biometals in the brain catalyze the formation of ROS, which further aggravates oxidative stress and thus, contributing to the AD pathogenesis.[34] Metal chelators can form complexes with these redox-active biometals and prevent the formation of ROS. The chelating abilities of the compound **5a** for the biologically relevant metal ions: Cu^{2+}, Fe^{3+} and Zn^{2+} were studied by UV-vis spectrometry. A series of UV-vis spectra of compound **5a** are demonstrated in the Figure 4. The absorbance spectra of **5a** showed a significant decrease after the addition of Cu^{2+}. An apparent red shift in the maximum absorption from 260 nm to 268 nm indicated an interaction between compound **5a** and Cu^{2+} due to complex formation.[35] Addition of Fe^{3+} or Zu^{2+} resulted minor changes in the UV

spectrum of **5a** indicating poor chelating capacity of the compound **5a** for Fe^{3+} or Zu^{2+} ion. Similar results were observed for the compounds **5b-d** (Fig. 4, B-D).

The stoichiometry of the **5a**-Cu^{2+} complex was determined using the molar ratio method, by preparing solutions of compound **5a** with increasing amounts of $CuCl_2$. The UV spectra were used to obtain the absorbance of the **5a** complex and differing concentrations of $CuCl_2$ at 373 nm. Two lines with different slopes were plotted to distal parts of the curve (approximations to tangents), with the interception at a molar ratio of 0.98 (Fig. 5), it revealed that a 1:1 stoichiometry for complex **5a**-Cu^{2+}. The complex formation constant (β_1) obtained after calculation is 1.10×10^6 $L\cdot mol^{-1}$, log β_1=6.04.

3.7 MTT assay of cell viability

Tacrine, a well-known AChE inhibitor, was withdrawn from the market for its severe reversible hepatotoxicity. Therefore, tacrine was used as the positive control. To determine whether our compounds had hepatotoxicity in comparison to tacrine, the representative compounds (**3a-d**, **5a-d**) were selected for the MTT assay in PC12 and HepG2 cell lines at the concentrations of 1, 10 and 100 μM, respectively. The results showed that the inhibition rates of all the tested compounds were less than 5% at 1 μM, and most of the compounds showed no obvious effect on cell viability at concentrations of 10 and 100 μM, as shown in the Table 2. The compounds exhibited lower toxicity towards the cell lines when compared with tacrine.

4. CONCLUSION

A series of genistein-*O*-alkylamine derivatives were synthesized and evaluated for multifunctional anti-AD agents. Among these compounds **3h-i** and **5e-i** were novel. The results showed that pyrrolidine modified derivatives (**3a-3d**, **5a-5d**) exhibited strong AChE inhibitory activity, and 7,4'-O-bis-substituted derivative **5a** exhibited the most potent inhibition with IC_{50} value of 0.034 μM. For BuChE inhibition, **5a** and **5c** were the most potent compounds with IC_{50} values of 0.33 and 0.35 μM, respectively. A Lineweaver-Burk plot and molecular modeling study suggested that the compound **5a** interacted with both the CAS and PAS of AChE, and induced a strong inhibition effect. Compound **5a** also displayed antioxidant activity with ORAC value of 1.21. The compounds **5a-5d** showed potent Cu^{2+} chelating ability. In addition, these compounds showed low toxicity towards PC12 and HepG2 cell lines by MTT assay *in vitro*. The results of the study showed that the compound **5a** is a potent, multifunctional, nontoxic drug and a suitable candidate for the treatment of AD.

ACKNOWLEDGEMENTS

We thank the Foundation of Henan Educational Committee (No. 182102310504, 14A350008), the Natural Science Foundation of China (No. U1704176, 81460528, 21762020), the Foundation for University Key Teacher by Educational Commission of Henan Province (2016GGJS-030), the Postdoctoral Science Foundation of China (No. 2012M521391), and the Postdoctoral Science Foundation of Henan Province (No. 2011015) for financial support of this study.

CONFLICT OF INTEREST

We declare that we have no conflict of interest.

List of the figure legends

Figure 1. Chemical structures of genistein and genistein derivatives.

Figure 2. Design strategy for the genistein derivatives.

Scheme 1. Synthesis of genistein derivatives. Reagents and conditions: (a) 1 equiv. $Br(CH_2)_nBr$, K_2CO_3, acetone, reflux; (b) 4 equiv. $Br(CH_2)_nBr$, K_2CO_3, acetone, reflux; (c) HNR_1R_2, K_2CO_3, CH_3CN, 60 °C.

Scheme 2. Synthesis of 4'-*O*-modified genistein derivatives **9a-b**. Reagents and conditions: (a) KOH, DMF, MOM-Cl, rt; (b) 1 equiv. $Br(CH_2)_4Br$, K_2CO_3, acetone, reflux; (c) HNR_1R_2, K_2CO_3, CH_3CN, 60 °C; (d) 10% HCl/EtOH, reflux.

Figure 3. Lineweaver-Burk plots (left) and docking model (right) for the compound **5a** with *Tc*AChE.

Figure 4. UV spectrum of compounds **5a-d** (20 μM) alone or at the presence of 20 μM Fe^{3+}, Cu^{2+} and Zn^{2+}.

Figure 5. Determination of the stoichiometry of complex-Cu^{2+} using the molar ratio method of titrating the methanol solution of **5a** with ascending amounts of $CuCl_2$. The final concentration of tested compound was 20 μM, and the final concentration of Cu^{2+} ranged from 2.0 to 200 μM.

REFERENCES

1. M. Townsend, *J. Alzheimers Dis.* **2011**, *24*, 43.
2. N. Khunnawutmanotham, N. Chimnoi, P. Saparpakorn, S. Techasakul, *Bioorg. Chem.* **2016**, *65*, 137.
3. S. S. Xie, X. B.Wang, J. Y. Li, L.Yang, L. Y. Kong, *Eur. J. Med. Chem.* **2013**, *64*, 540.
4. L. A. Craig, N. S. Hong, R. J. McDonald, *Neurosci*. *Biobehav. Rev*. **2011**, *35*, 1397.
5. B. Li, J. A. Stribley, A. Ticu, W. H. Xie, L. M. Schopfer, P. Hammond, S. Brimijoin, S. H. Hinrichs, O. Lockridge, *J. Neurochem*. **2000**, *75*, 1320.
6. D. Knez, B. Brus, N. Coquelle, I. Sosic, R. Sink, X. Brazzolotto, J. Mravljak, J. P. Colletier, S. Gobec, *Bioorg. Med. Chem.* **2015**, *23*, 4442.
7. A. Cavalli, M. L. Bolognesi, A. Minarini, M. Rosini, V. Tumiatti, M. Recanatini, C. Melchiorre, *J. Med. Chem.* **2008**, *51*, 347.
8. L. Huang, C. Lu, Y. Sun, F. Mao, Z. Luo, T. Su, H. Jiang, W. Shan, X. Li, *J. Med. Chem.* **2012,** *55*, 8483.
9. X. K. Li, H. Wang, Z. Y. Lu, X. Y. Zheng, W. Ni, J. Zhu, Y. Fu, F. L. Lian, N. X. Zhang, J. Li, H. Y. Zhang, F. Mao, *J. Med. Chem.* **2016,** *59*, 8326.
10. M. A. Santos, K. Chand, S. Chaves, *Coord. Chem. Rev.* **2016**, *327*, 287.
11. A. S. Darvesh, R. T. Carroll, A. Bishayee, W. J. Geldenhuys, C. J. Van der Schyf, *Expert. Rev. Neurother.* **2010**, *10*, 729.
12. H. J. Lee, K. J. Korshavn, A. Kochi, J. S. Derrick, M. H. Lim, *Chem. Soc. Rev.* **2014**, *43*, 6672.
13. P. B. Kaufman, J. A. Duke, H. Brielmann, J. Boik, J. E. Hoyt, *J. Altern. Complement. Med.* **1997**, *3*, 7.
14. A. A. Ganai, H. Farooqi, *Biomed. Pharmacother.* **2015**, *76*, 30.
15. O. Y. Bang, H. S. Hong, D. H. Kim, H. Kim, J .H. Boo, K. Huh, I. Mook-Jung, *Neurobio. Dis.* **2004**, *16*, 21.
16. M. Bagheri, M. T. Joghataei, S. Mohseni, M. Roghani, *Neurobiol. Learn. Mem.* **2011**, *95*, 270.
17. D. H. Shi, Z. Q. Yan, L. N. Zhang, Y. R. Wang, C. P. Jiang, J. H. Wu, *Arch. Pharm. Res.* **2012**, *35*, 1645.
18. X. Qiang, Z. Sang, W. Yuan, Y. Li, Q. Liu, P. Bai, Y. Shi, W. Ang, Z. Tan, Y. Deng, *Eur. J. Med. Chem.* **2014**, *76*, 314.
19. W. Luo, Y. P. Li, Y. He, S. L. Huang, J. H. Tan, T. M. Ou, D. Li, L. Q. Gu, Z. S. Huang, *Bioorg. Med. Chem.* **2011**, *19*, 763.
20. C. Hong, W. Luo, D. Yao, Y. B. Su, X. Zhang, R. G. Tian, C. J. Wang, *Bioorg. Med. Chem.* **2014**, *22*, 3213.
21. W. Luo, T. Wang, C. Hong, Y. C. Yang, Y. Chen, J. Cen, S. Q. Xie, C. J. Wang, *Eur. J. Med. Chem.* **2016**, *122*, 17.
22. X. Zhang, J. Wang, C. Hong, W. Luo, C. Wang, *Acta Pharm. Sin. B.* **2015**, *5*, 67.
23. W. Luo, Y. B. Su, C. Hong, R. G. Tian, L. P. Su, Y. Q. Wang, Y. Li, J. J. Yue, C. J. Wang, *Bioorg. Med. Chem.* **2013**, *21*, 7275.
24. W. Luo, Y. Chen, T. Wang, C. Hong, L. P. Chang, C. C. Chang, Y. C. Yang, S. Q. Xie, C. J. Wang, *Bioorg. Med. Chem.* **2016**, *24*, 672.
25. Y. Deng, Z. Tan, X. Qiang, W. Yuan, Z. Sang, Q. Liu, Y. Li, Patent WO2014111028A1, **2014**.
26. G. L. Ellman, K. D. Courtney, V. Jr. Andres, R. M. Feather-Stone, *Biochem. Pharmacol.* **1961**, *7*, 88.
27. P. T. Lewis, K. Wahala, A. Hoikkala, I. Mutikainen, Q. H. Meng, H. Adlercreutz, M. J. Tikkanen, *Tetrahedron.*

2000, *56*, 7805.

28. S. B. R. Castro, C. O. R. Junior, C. C. S. Alves, A. T. Dias, L. L. Alves, L. Mazzoccoli, M. T. Zoet, S. A. Fernandes, H. C. Teixeira, M. V. Almeida, A. P. Ferreira, *Chem. Biol. Drug Des.* **2012**, *79*, 347.
29. X. M. Qiang, W. Yuan, Z. P. Sang, Y. Deng, *Chinese J. Org. Chem.* **2013**, *33*, 621.
30. P. Anand, B. Singh, *Arch. Pharm. Res.* **2013**, *36*, 375.
31. R.M. Lane, S.G. Potkin, A. Enz, *Int. J. Neuropsychopharmacol.* **2006**, *9*, 101.
32. G.M. Morris, D.S. Goodsell, R.S. Halliday, R. Huey, W.E. Hart, R.K. Belew, A.J. Olson, *J. Comput. Chem.* **1998**, *19*, 1639.
33. W.L. DeLano, The PyMOL Molecular Graphics System. DeLano Scientific: San Carlos, CA. 2002.
34. A. I. Bush, *J. Alzheimers Dis.* **2008**, *15*, 223.
35. M. L. Bolognesi, A. Cavalli, L. Valgimigli, M. Bartolini, M. Rosini, V. Andrisano, M. Recanatini, C. Melchiorre, *J. Med. Chem.* **2007,** *50*, 6446.

Table 1. Inhibition of AChE, BuChE and oxygen radical absorbance capacity (ORAC, Trolox equivalents) of the compounds.

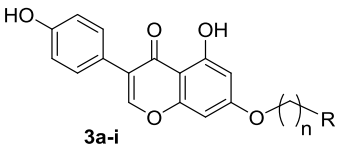

3a-i

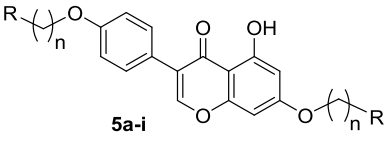

5a-i

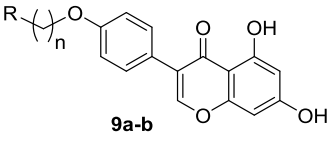

9a-b

Compd.	R	n	IC_{50}[a] for AChE (μM)	IC_{50}[b] for BuChE (μM)	Selectivity for AChE[c]	ORAC[d]
3a		2	0.56±0.03	1.37±0.08	2.4	1.85±0.14
3b		3	1.11±0.17	6.48±0.42	5.8	1.94±0.10
3c		4	0.44±0.01	3.90±0.26	8.9	1.42±0.06
3d		6	0.88±0.12	1.21±0.11	1.4	1.15±0.08
3e		2	>10	>10	-	2.31±0.06
3f		3	>10	>10	-	2.13±0.04
3g		4	>10	>10	-	1.58±0.11
3h		6	>10	>10	-	2.04±0.09
3i		8	>10	>10	-	1.39±0.17
5a		2	0.034± 0.003	0.33±0.05	9.7	1.21±0.07
5b		3	0.29±0.02	0.61±0.10	2.1	1.02±0.03
5c		4	0.08±0.01	0.35±0.08	4.4	0.65±0.12
5d		6	0.31±0.04	0.58±0.02	1.9	0.78±0.05

5e		2	0.42±0.03	>10	>23.8	1.10±0.02
5f		3	2.43±0.06	8.12±0.57	3.3	1.23±0.07
5g		4	>10	>10	-	0.56±0.02
5h		6	>10	>10	-	0.62±0.03
5i		8	>10	>10	-	0.70±0.10
GS-14		4	0.29±0.03	>10	>34.5	2.15±0.08
9a		4	4.98±0.35	>10	>2.0	1.49±0.03
9b		4	7.25±0.52	>10	>1.4	1.32±0.05
Genistein	-	-	>100	>100	-	4.20±0.23
Donepezil	-	-	0.037± 0.002	7.76±0.36	209.7	<0.2
Rivastigmine	-	-	6.53±1.30	1.41±0.08	0.2	<0.2

[a] AChE from *electric eel*; IC_{50}, 50% inhibitor concentration (means ± SEM of three experiments).

[b] BuChE from *equine serum*; IC_{50}, 50% inhibitor concentration (means ± SEM of three experiments).

[c] Selectivity ratio =IC_{50} (BuChE)/ IC_{50} (AChE).

[d] Data are expressed as (μmol trolox)/(μmol tested compound).

Table 2. The inhibition ratios of compounds towards PC12 and HepG2 cell lines [a]

Compd.	PC12 (%)			HepG2 (%)		
	1 μM	10 μM	100 μM	1 μM	10 μM	100 μM
3a	<5	8.23±0.21	14.68±1.30	<5	6.27±1.42	9.45±1.08
3b	<5	6.52±0.76	23.71±0.93	<5	<5	16.84±2.55
3c	<5	<5	<5	<5	9.02±0.77	24.11±2.19
3d	<5	10.24±0.85	18.05±2.30	<5	<5	10.39±0.57
5a	<5	<5	12.47±1.83	<5	8.72±0.35	17.65±1.31
5b	<5	<5	9.12±0.88	<5	<5	<5
5c	<5	5.74±0.35	16.21±1.02	<5	<5	8.38±0.12
5d	<5	7.42±0.66	19.22±2.31	<5	<5	20.88±3.53
Tacrine	<5	14.20±0.34	24.32±2.11	<5	18.92±1.49	37.55±4.72

[a] The inhibitory rates were determined at three different concentrations. Data are presented as the mean ± SD of three independent experiments.